NORMAL AND HIGH-STRENGTH R/C DEEP BEAMS UNDER PURE TORSION AND CODES EVALUATION

دراسة سلوك اللي للكمرات العميقة من الخرسانة المسلحة العادية والعالية المقاومة وتقييم متطلبات الكودات

Ahmed M. Yousef

Associate Prof., Structural Eng. Department, Faculty of Eng., Mansoura University, Egypt

خلاصة:

يقدم هذا البحث نتائج تجارب معملية أجريت على عدد ١٤ كمرة عميقة في اللي وذلك لتقييم مدى إمكانية تطبيق متطلبات التصميم فى اللي والواردة فى أربعة من الكودات الدولية (هي الكود الأمريكي والكود المصري والكود النيوزيلاندي والكود الأوربي الثاني) عند تطبيقها على الكمرات العميقة المصنعة من الخرسانة عالية المقاومة. وقد تم استخدام نتائج هذه التجارب لإجراء مقارنة بين سلوك اللي للكمرات العميقة المصنعة من الخرسانة.عالية المقاومة والتي لها مقاومة ضغط للمكعب حوالي ٨١ ميجاباسكال مع تلك المصنعة من الخرسانة عادية المقاومة والتي لها مقاومة ضغط للمكعب حوالي ٣٥ ميجاباسكال. وأهم المتغيرات التي تم دراستها هي مقاومة الضغط التصميمية للخرسانة و نسبة التسليح العرضي ونسبة الحديد الطولي للكمرة بالإضافة إلى مقاس للكمرات المختبرة على شكل نسبة البحر المختبر للعمق. وقد أوضحت النتائج أن الاحتياطي الموجود في مقاومة اللي يكون أقل كثيرا في الكمرات العميقة العالية المقاومة عن مثيلتها المصنعة من خرسانة عادية المقاومة. كما تبين أن مقاومة الشروخ في اللي للكمرات العميقة عادية المقاومة بلغت ٣٨-٥٤% من مقاومة اللي القصوى في حين أن هذه النسبة للكمرات العميقة المماثلة من الخرسانة عالية المقاومة كانت حوالي ٥٧-٧٧%. وقد أظهرت النتائج أن معادلات حساب المقاومة القصوى في اللي للكمرات العميقة الواردة في الكودات الأربعة التي تم دراستها في هذا البحث كانت آمنة عند تطبيقها على الكمرات العميقة من الخرسانة العادية و العالية المقاومة. كما أوضحت النتائج أن استخدام معادلات الكود الأمريكي مع أخذ قيمة زاوية ميل العصب الخرساني على المحور الطولي للكمرة مساوية ٤٥ درجة قد تعطي نتائج أقل أمان منها في حالة أخذ هذه الزاوية بين ٣٠-٦٠ درجة.

ABSTRACT

Fourteen reinforced concrete deep beams were tested under pure torsion in order to evaluate the torsion design provisions of ACI 318-02 Building Code, the Egyptian code (ECCS-2001), the New Zealand code (NZS 3101-95), and the Eurocode 2 (EC-2) when applied to High-Strength Concrete (HSC) deep beams. The results of these tests have been used to compare the torsional behavior of reinforced deep beams constructed from Normal-Strength Concrete (NSC with characteristic cube compressive strength f_{cu} of about 35 MPa) and HSC (with f_{cu} of about 81 MPa). The main parameters examined in this study were the design compressive strength, the provided transverse reinforcement ratio, the quantity of longitudinal and skin reinforcement and the size of the tested beams in the form of the tested span to total height ratio (L/h=1.0, 2.0 and 3.0). The results showed that the reserve in the torsional strength of the HSC deep beams after cracking is considerably less than that of the similar NSC deep beams. The cracking torsional strength of the tested NSC deep beams is about 38-54% of the measured ultimate torsional strength, while the same ratio for the similar HSC deep beams is about 57-77% of the measured ultimate strength. The design torsional strength equations of the four international codes considered in this study were safe and conservative when applied to NSC and HSC deep beams. The predictions of the ultimate torsional strength of the deep beams according to the method of ACI 318-02 and using a value of the angle between the concrete struts and the longitudinal axis of the beam θ equal to 45 deg may give a conservative results less than that calculated using this angle between 30 and 60 deg.

1. INTRODUCTION

For many years, concrete with compressive strength in excess of 40 MPa was available at only a few locations. However, in recent years, the applications of High-Strength Concrete (HSC) have increased, and HSC with compressive strength approaching 140 MPa, has now been used in many parts of the world [1]. The growth has been possible as a result of recent developments in material technology. The main advantage of using HSC is the cost saving from the use of lower volumes of concrete which results in reduced shuttering costs and lighter foundations [1].

Deep beams are characterized by relatively small values of span to depth ratios. Because of their proportions, they develop mechanism of force transfer quite different from that in shallow beams. Until now, there is no unified definition for the deep beams. According to the ACI-ASCE Committee 326 [2], a beam with shear span-to-depth ratio (a/d) less than 1.0 is classified as deep beam, and a beam with a/d exceeding 2.5 as an ordinary shallow beam. Any beam in between these two limits is classified as a short beam. According to the New Zealand code for design of concrete structures (NZS 3101-95) [3] a simple beam with a/d less than 2 is classified as deep beam. The Eurocode 2 (EC-2) [4] defines the simple beam with total clear span-to-depth ratio (L_n/d) less than 2 as deep beam. Deep beams in ACI 318 building code (ACI 318-02) [5] refer to beams with (L_n/d) ratio less than 5.0. According to the Egyptian code for design of concrete structures (ECCS-2001) [6] a simple beam with effective span to depth ratio less than 1.25 is considered as a deep beam. For the analysis and design of shallow and deep reinforced NSC beams, most of the available codes adopted the rational thin-walled tube space truss model [3-6]. Recently, Rahal and Collins [7] tested four beams constructed from NSC to evaluate the torsion design procedures of ACI 318-02 and AASHTO-LRFD. The

only reported study on the torsional behavior of HSC deep beams has been published by Ashour et al. [8]. The studied parameters were the concrete compressive strength and the span-to-depth ratio.

The main objective of this paper is to examine the applicability of the torsion design provisions of the ACI 318-02 building code, ECCS-2001, NZS 3101-95 and EC-2 when applied to HSC deep beams. The results of these tests have been used to compare the torsional behavior of reinforced NSC and HSC deep beams.

2. CRACKING AND ULTIMATE TORSIONAL STRENGTH OF R/C DEEP BEAMS ACCORDING TO THE CODES PROVISIONS

2.1 Cracking Torsional Strength

For calculating the cracking torsional moment T_{cr}, the NZS 3101-95, ACI 318-02 Building Code and ECCS-2001 use the following equation:

$$T_{cr} = 0.33 \left(\frac{A_{cp}^2}{P_{cp}}\right)\sqrt{f_c'} \qquad (1)$$

where A_{cp} is the gross area bounded by outer perimeter of concrete cross-section, p_{cp} is the outer perimeter of concrete cross-section and f_c' is the design cylinder compressive strength. The EC-2 does not give an equation for calculating the cracking torsional strength.

2.2 Ultimate Torsional Strength

ACI 318-02

The nominal torsional stress, v_{tn}, can be calculated from the following equation:

$$v_{tn} = \frac{T_n}{2A_o t_e} \qquad (2)$$

where T_n is the nominal torsional moment, t_e is the wall thickness of the equivalent thin-walled tube at the point where the shear stress, v_{tn}, due to torsion is

being computed; A_o is the cross-sectional area bounded by the centerline of the shear flow. The area A_o is empirically taken as 0.85 times the area A_{oh} enclosed by the outermost closed stirrups in the section, and t_e is taken as (A_{oh}/p_h) where p_h is the perimeter of the centerline of the closed stirrups. The ultimate torsional moment T_u usually taken less than or equal to (φT_n), where φ is the strength reduction factor.

If the ultimate shear stress, v_{tu}, induced by torsion as calculated from Eq. (1) is less than a minimal value v_{tnMIN}, the torsional effects may be neglected. The maximum ultimate torsional shear stresses v_{tnMAX} are limited also by the ACI 318-02 regardless of the amount of reinforcement to safeguard against wide cracks and large deformations. The minimum and maximum values of v_{tu} allowed by the code are given in the form of a ratio of square root of the design cylinder compressive strength of concrete as follows:

$$v_{tnMIN} = 0.08 \sqrt{f_c} \quad MPa \qquad (3)$$

$$v_{tnMAX} = 0.66 \sqrt{f_c} \quad MPa \qquad (4)$$

If the ultimate shear stress induced by torsion is greater than the minimum value and less than the maximum value given by Eq. (4), reinforcement for torsion must be provided. The torsional reinforcement must consist of closely spaced well-anchored stirrups and of additional longitudinal bars. The following equations are used:

$$A_t = \frac{T_n \cdot s}{2 A_o f_{yv} \cot \theta} \qquad (5)$$

$$A_l = \frac{T_n p_h}{2 A_o f_{yl}} \cot \theta \qquad (6)$$

$$\cot \theta = \sqrt{\frac{A_l f_{yl} s}{A_t f_{yv} p_h}} \qquad (7)$$

where A_t is the area of one stirrup leg, f_{yv} is the yield stress of stirrup's steel not to exceed 400 MPa, s is the spacing between stirrups, θ is the angle between the concrete struts and the longitudinal axis of

the beam and shall not be taken smaller than 30 deg nor larger than 60 deg. A_l is the area of the required additional longitudinal reinforcement and f_{yl} is the yield stress of the longitudinal bars. According to this code, the angle θ can be taken equal 45 deg for nonprestressed members. For convenience in design, A_l, can be expressed in terms of the area of the torsional stirrups:

$$A_l = \frac{A_t f_{yv} p_h}{s f_{yl}} \cot^2 \theta \qquad (8)$$

The minimum area of one leg of stirrup for torsion is given as follows:

$$A_t = \frac{0.17 s \cdot b}{f_{yv}} \qquad (9)$$

where b is the breadth of the beam cross-section. The spacing between the transverse torsion reinforcement shall not exceed the smaller of 300 mm or $(P_h/8)$. The minimum longitudinal reinforcement should be calculated from the following expression:

$$A_{slmin} = \left(\frac{0.41 A_{cp} \sqrt{f_c}}{f_{yl}}\right) - \left(\frac{A_t p_h f_{yv}}{s f_{yl}}\right) \qquad (10)$$

The longitudinal reinforcement required for torsion shall be distributed around the perimeter of the closed stirrups with a maximum spacing of 300 mm. There shall be at least one longitudinal bar in each corner of the stirrups. The minimum diameter of the additional longitudinal bars shall be 10 mm or 1/15 of the spacing between stirrups whichever is larger.

ECCS-2001

The torsional provisions of reinforced concrete beams in this code is almost the same as that in ACI 318-02. However, some differences are found as will be shown next. The ultimate torsional shear stress, v_{tu}, due to ultimate torsional

moment T_u is given by an equation similar to Eq. (2). The minimum and the maximum values of v_{tu} are given as follows:

$$v_{tu\,MIN} = 0.06 \sqrt{\frac{f_{cu}}{\gamma_c}} \qquad (11)$$

$$v_{tu\,MAX} = 0.70 \sqrt{\frac{f_{cu}}{\gamma_c}} \qquad (12)$$

where γ_c is the partial safety factor for concrete which is taken equal to 1.5.

The ECCS-2001 assumes that for reinforced concrete members the angle θ is 45 deg throughout. Equations 5 and 6 are modified as follow:

$$A_t = \frac{T_u . s}{2 A_o (f_{yv} / \gamma_s)} \qquad (13)$$

$$A_l = \frac{T_u p_h}{2 A_o (f_{yl} / \gamma_s)} \qquad (14)$$

where γ_s is the partial safety factor for reinforcement steel which is taken equal to 1.15.

The minimum closed stirrup reinforcement for torsion and the minimum longitudinal torsion reinforcement is approximately the same as that given in the ACI 318-02 (Eq. 9 and Eq. 10). The spacing s shall not exceed the smaller of 200 mm or $(P_h/8)$. The diameter of the longitudinal bars should not be less than 12 mm or $(s/15)$ whichever is larger.

NZS 3101-95

The nominal torsional stress, v_{tn}, can be calculated from the following equation:

$$v_{tn} = \frac{T_n}{2 A_{oc} t_{oc}} \qquad (15)$$

where t_{oc} is the wall thickness of the equivalent thin-walled tube and A_{oc} is the cross-sectional area enclosed by the line connecting the centers of longitudinal bars in the corners of the stirrups. The value of t_{oc} is taken as $(0.75A_{oc}/p_{oc})$ where p_{oc} is the perimeter of A_{oc}. The value of v_{tn} shall not exceed $(0.2 f_c)$ or 6 MPa. The minimum nominal torsional stress required by this code is the same as that given in Eq. (3).

The required area of closed stirrups A_t and the required A_l can be calculated as follows (with θ equal to 45 deg):

$$A_t = \frac{T_n . s}{2 A_{oc} f_{yv}} \qquad (16)$$

$$A_l = \frac{T_n p_{oc}}{2 A_{oc} f_{yl}} \qquad (17)$$

The minimum amount of stirrups and longitudinal bars shall be provided such that:

$$\sqrt{\frac{A_t}{s} . \frac{A_l}{p_{oc}}} \geq \frac{1.5}{f_{yv}} . \frac{A_{cp} t_c}{A_{oc}} \qquad (18)$$

where t_c shall be taken equal to $(0.75A_{cp}/p_{cp})$. The minimum requirements for longitudinal bars is the same as that in ACI 318-02. The spacing between the transverse torsion reinforcement shall not exceed the smaller of 300 mm or $(P_{oc}/8)$.

EC-2

The design ultimate torsional moment T_u should not be greater than T_{Rd1} and T_{Rd2} where T_{Rd1} is the maximum torsional moment that can be resisted by the compression struts in the concrete and T_{Rd2} is the maximum torsional moment that can be resisted by the stirrups. The values of T_{Rd1} and T_{Rd2} can be calculated from the following equations:

$$T_{Rd1} = T_{uc} = \frac{2 \, v \, t_o \, A_k \, f_{cd}}{(cot\theta + tan\theta)} \qquad (19)$$

$$T_{Rd2} = T_{ul} = \frac{2 A_k A_l f_{yl} \, cot\theta}{s} \qquad (20)$$

where t_o is the equivalent thickness and should be taken less than or equal to (A_{cp}/p_{cp}), A_k is the area enclosed within the center line of the equivalent thin-walled section and p_k is the perimeter of the area A_k. The angle θ can be calculated using Eq. (6). The EC-2 requires that the angle θ should be taken so that

$$|0.4| \le cot\theta \le |2.5| \qquad (21)$$

The efficiency factor v can be calculated from the following equation:

$$v = 0.7 \, [0.7 - (f_{ck}/200)] \ge 0.35 \qquad (22)$$

where f_{ck} is the characteristic cylinder compressive strength of concrete at 28 days. The design cylinder compressive strength of concrete f_{cd} is equal to f_{ck} divided by γ_c (γ_c is the partial safety factor for concrete which is taken equal to 1.5).

The ultimate torsional moment depending on the torsional strength of the longitudinal bars T_{ul} can be calculated as follows:

$$T_{ul} = \frac{2 A_o A_l f_{yl}}{p_h \, cot\theta} \qquad (23)$$

The spacing between the torsion stirrups shall not exceed the smaller of 200 mm or $(P_k/8)$. The diameter of the longitudinal bars should not be less than 12 mm and the distance between these bars should not exceed 350 mm. The EC-2 did not exactly define the area A_k and the perimeter p_k. In this study, the area A_k will be taken equal to that recommended by the ACI 318-02 as 0.85 times the area A_{oh} enclosed by the centerline of outermost closed stirrups in the section and p_k is the perimeter of A_{oh}.

3. EXPERIMENTAL PROGRAM

3.1 Details of the Tested Deep Beams

The test specimens consisted of fourteen reinforced concrete beams with web reinforcement divided into 2 groups. The first group consists of 7 NSC deep beams and the second group consists of seven similar HSC deep beams. All the tested beams have the same rectangular cross-section of 125 mm wide and 450 mm total height. A concrete cover of 20 mm was used. It should be noted that, all the tested beams are classified as deep beams according to ACI 318-02 building code. The beams subjected to torsion can be classified according to the provided reinforcement into the following three cases: 1) over-reinforced, when crushing of concrete takes place before yielding of both stirrups and longitudinal bars; 2) under-reinforced, when both the stirrups and the longitudinal bars yield before crushing of the concrete diagonals; 3) partially over-reinforced, when either stirrups or longitudinal bars, but not both, yield before crushing of concrete diagonals. The torsion provisions of the studied codes are based on under-reinforced sections. Most of the tested beams can be considered torsionally under-reinforced as will be explained in the next sections. Table 1 summarizes the details of the test program, while the reinforcement arrangement and dimensions of the tested beams are shown in Fig. 1. The main parameters considered are:

1. The tested span to total height ratio (L/h). Three L/h ratios were tested ($L/h= 1$, 2 and 3), and the tested span for the beams was equal to 450, 900 and 1350 mm, respectively.

2. Two different spacing between stirrups (100 mm and 200 mm) were tested. The diameter of the stirrups d_v was the same for all the tested beams ($d_v = 6$ mm). The provided stirrups cover the requirements of

was held against torsional rotation. The details of the loading arrangement are shown in the schematic illustration in Fig. 2. The clear span of the tested deep beams was changed according to the tested (*L/h*) ratio. Electrical strain gauges were bonded to the longitudinal torsional reinforcement, the skin reinforcement and the stirrups at

some locations as shown in Fig. 1. The load was applied with increments up to failure at a distance of 225 mm from the longitudinal centerline of the tested deep beam. At each load increment, torsional rotations at the free end of the deep beam were recorded. The test setup is shown from the photograph in Fig. 3.
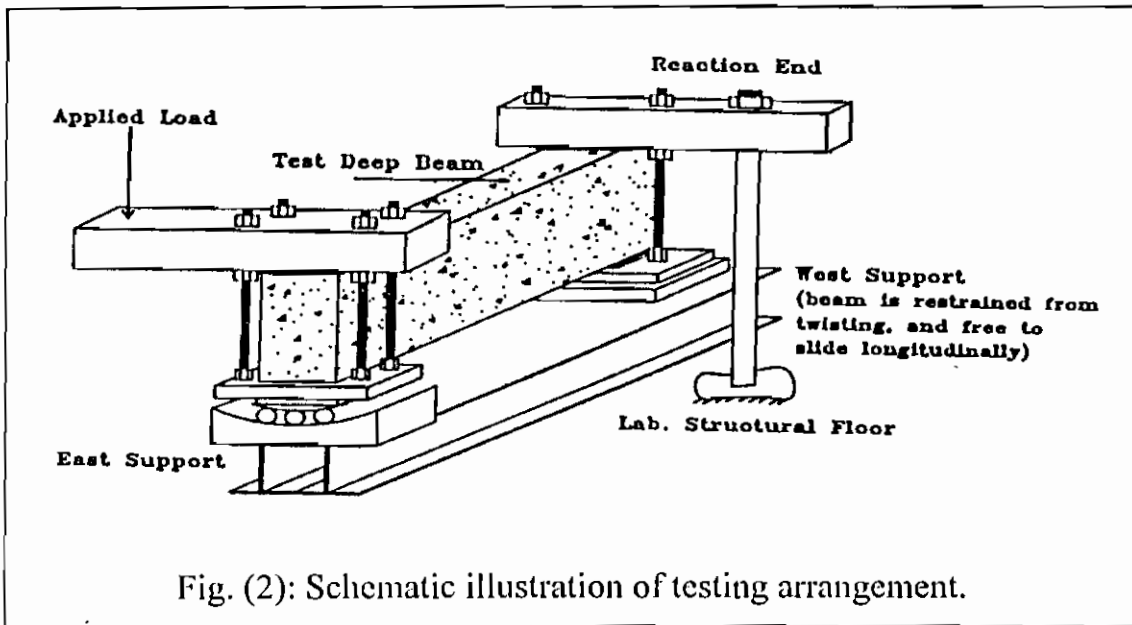
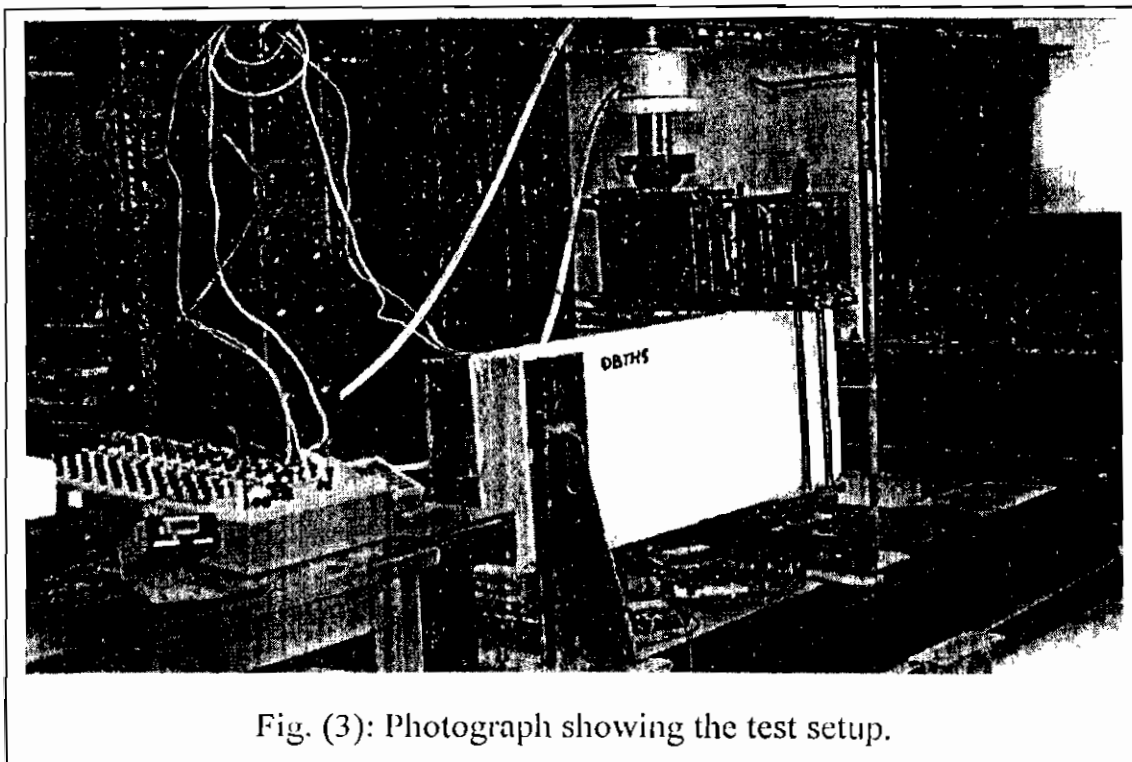Fig. (2): Schematic illustration of testing arrangement.

Fig. (3): Photograph showing the test setup.

4. ANALYSIS OF TEST RESULTS

4.1 Applied Torsional Moment-Strain Relationships

The recorded strain readings in the upper longitudinal reinforcement on the middle of the tested span of the beams and in the legs of the middle stirrups for some of the tested specimens are plotted in Fig. 4 and 5, respectively, versus the applied torsional moment. The results of the tests indicate that, the strains in the longitudinal and in the transverse reinforcement before the initial concrete cracking were very small. A sudden high increase in the strains took place after the formation of the first spiral crack. Following this, the tensile steel strains in the stirrups and the longitudinal bars increased at a faster rate up to yielding. As can be seen from Fig. 4a, comparing the strains recorded in the transverse reinforcement of the tested HSC and NSC deep beams showed that increasing the concrete strength for the same reinforcement reduced considerably the strains at the same torsional moment. The strains recorded in the stirrups of deep beams DBTN2, DBTN3 and DBTN4 were considerably more than that of beams DBTH2, DBTH3 and DBTH4, respectively. Yielding of the stirrup's legs in the tested HSC and NSC beams did not have any considerable observed indication on the spiral cracks. For the similar HSC and NSC deep beams, increasing the spacing between the stirrups increases the recorded strains in the stirrups. For all the tested deep beams, yielding of the stirrups was attained before yielding of the longitudinal bars or crushing of the concrete. This was because in all the tested deep beams, the provided stirrups covers, by a small percentages, the minimum requirements of the codes. For the similar HSC and NSC deep beams, increasing the L/h ratio increased considerably the

recorded strains in the stirrups. As can be seen from Fig. 4.b, the strains recorded in the stirrups of beam DBTH7 (L/h=3.0) were considerably larger than that of the similar beam DBTH2 but with (L/h=1.0).

From Fig. 5a, it can be seen that the recorded strains at the same load for NSC beams were larger than the similar beams constructed from HSC. Failure of the HSC beams was controlled by the amount of the strain in the longitudinal bars. This was observed especially for all the tested HSC beams regardless of the amount of stirrups. Increasing the strain in the longitudinal bars gradually increases the main spiral crack width, and at yielding of these bars the beam forms a torsional hinge at the yield/spiral crack location. For HSC beams, crushing of concrete at the torsional hinge region took place at a torsional moment generally larger than the torsional moment at yielding of the longitudinal bars. For NSC specimens, crushing of the concrete may take place at high strain levels in the longitudinal bars but before yielding of these bars as can be seen from Fig. 5b for beams DBTN1, DBTN2 and DBTN7. Increasing the L/h ratio for the similar HSC and NSC deep beams, increased the recorded strains in the longitudinal corner bars.

4.2 Cracking Behavior and Torsional Strength

The recorded values of the cracking and ultimate torsional moment and corresponding angle of twist are summarized in Table 2. Upon comparing the deep beams of the same reinforcement details constructed from NSC and HSC, it is obvious that, increasing the concrete strength considerably increases the value of the cracking torsional moment. Before the formation of cracks, the behavior of the beams under pure torsion was initially elastic. In this case, torsion is mainly resisted by concrete.
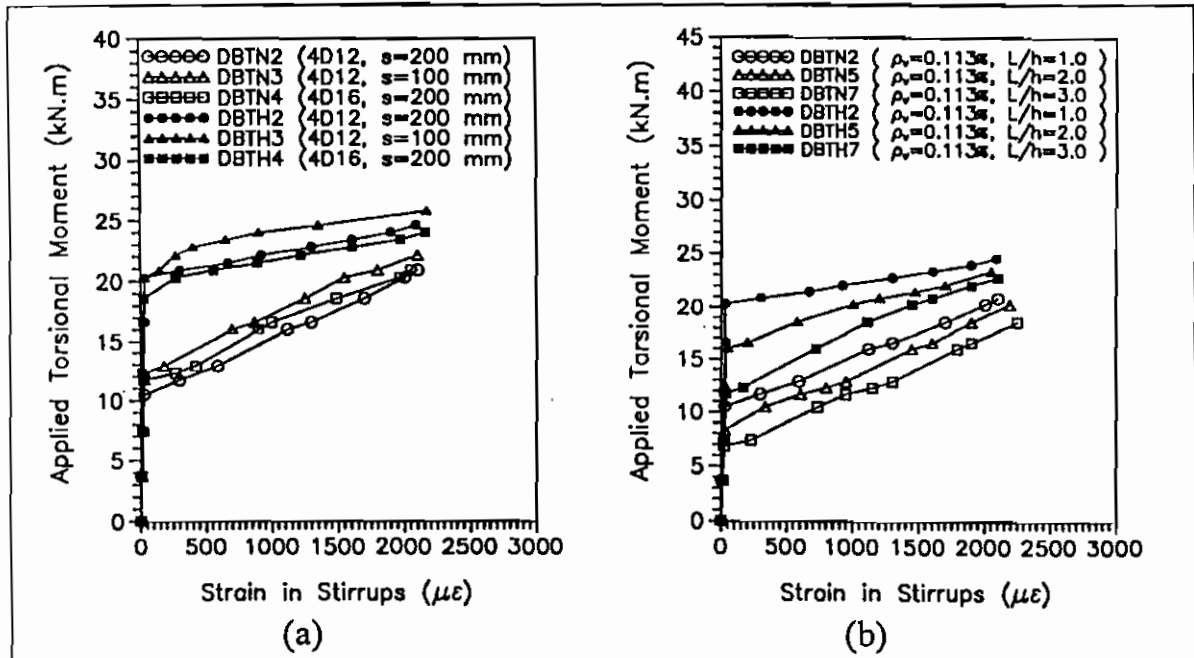
Fig. (4): Experimental torsional moment-stirrups strains
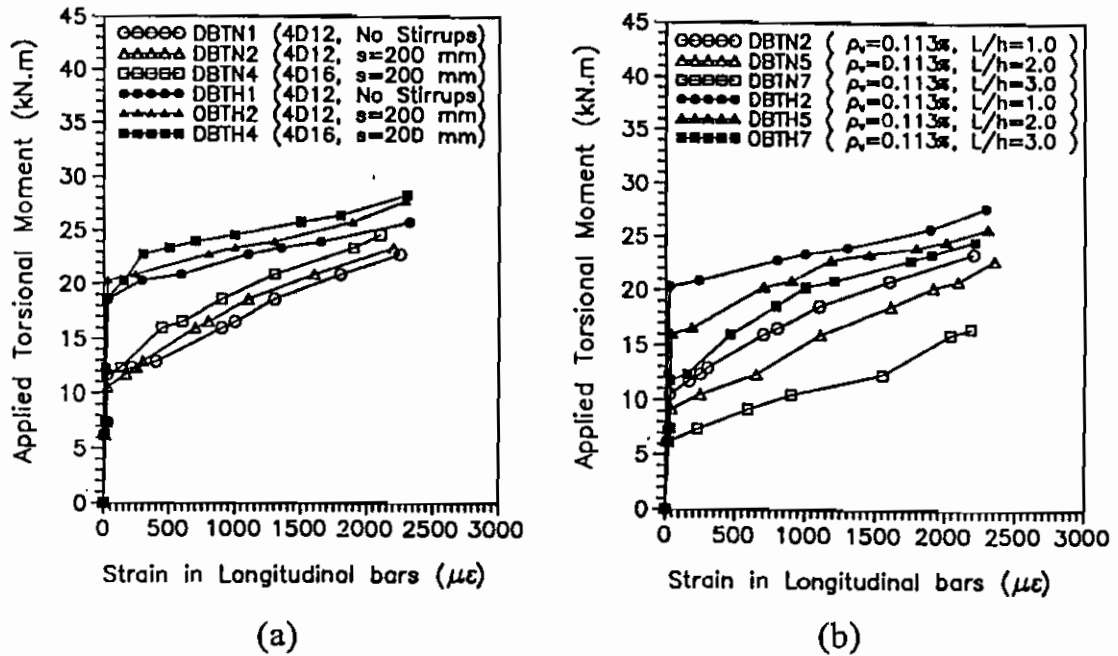relationships for the tested deep beams.

Fig. (5): Experimental torsional moment-longitudinal steel strains
relationships for the tested deep beams.

Increasing the spacing between the stirrups or the diameter of the longitudinal bars or existence of skin bars did not have a considerable effect on the cracking torsional moment. The recorded cracking torsional moments of the tested HSC deep beams were larger than that of the similar NSC beams by 58-79%.

The percentages of increase in the ultimate torsional strength were greatly less than the percentage of increase of the cracking torsional strength. The recorded ultimate torsional moment of the HSC deep beam DBTH5 was larger than that of DBTN5 by 10%, while the recorded ultimate torsional moment of DBTH7 was larger than that of DBTN7 by 25%. Increasing the L/h ratio reduces considerably both the cracking and ultimate torsional strength of the tested NSC and HSC deep beams. For the tested NSC beams, increasing the L/h ratio from 1 to 3 (DBTN2 and DBTN7) reduced the cracking and the ultimate torsional strength by 37% and 28%, respectively, while for the tested HSC deep beams, increasing the L/h ratio from 1 to 3 (DBTH2 and DBTH7) reduced the cracking and the ultimate torsional strength by 41% and 22%, respectively. It can be seen from Table 2 that, the cracking torsional strength of the tested NSC deep beams is about 38-54% of the measured ultimate torsional strength, while the same ratio for HSC deep beams is about 57-77% of the measured ultimate strength. This result showed that the reserve in the torsional strength of the tested HSC deep beams after cracking is relatively less than that of the similar NSC deep beams. This can be attributed to the brittle nature of the HSC. While the applied torsional moment increases, the appearance and progress of diagonal cracks up and down on the longer sides of the cross-section increases forming a spiral around the beam which spreads over the test regions. The spiral cracks angle with respect to the horizontal plane of the beam were between 30 to 55 deg for all the tested
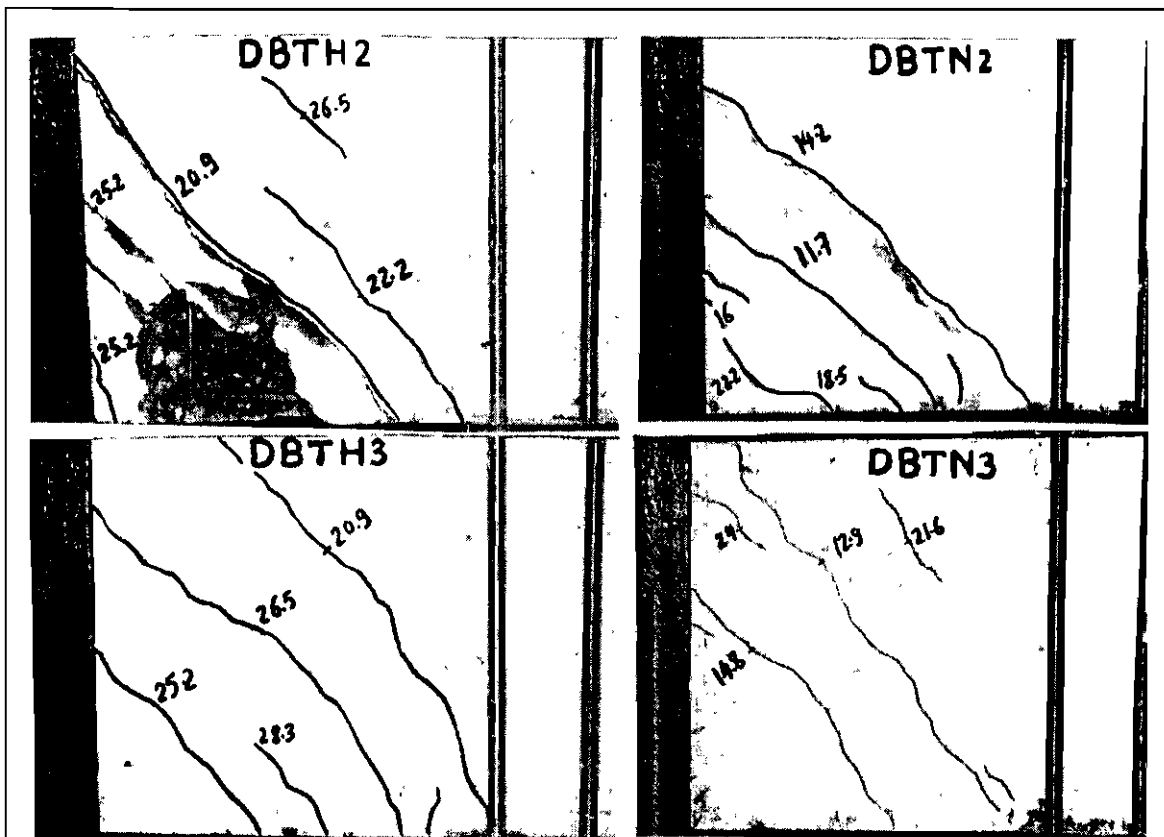
beams. Photographs of the crack patterns at failure for some of the tested beams with L/h=1 and 2 are shown in Figs. 6 and 7, respectively. The numbers written along the cracks on the photographs indicate the torsional moment (in kN.m) at termination of cracks observed at the end of a particular load stage.

The crack patterns of the tested deep beams with L/h=1 were approximately similar, as can be seen from the photographs in Fig. 6, despite that the stirrups ratio was different (ρ_v%= 0.0, 0.113 and 0.226). This can be attributed to the tested very short span. The crack patterns of the tested HSC and NSC deep beams with L/h=2 and 3 were essentially based on the L/h ratio and the spacing between the stirrups of the deep beams. Reducing the L/h ratio and increasing the spacing between the stirrups resulted in a few number of spiral cracks for HSC and NSC deep beams as can be seen from the photographs in Fig. 7 for beam DBTH5 and DBTN5 which experienced only 2 major cracks, while beams DBTH6 and DBTN6 experienced several cracks over the tested region. The existence of the skin bars in beams DBTN4 and DBTH4 did not have observed effect on the number of the torsional cracks.

The observed failure of the tested NSC and HSC deep beams was mainly controlled by the yielding of the longitudinal reinforcement. Whereas the applied torsional moment approaches the ultimate torsional capacity of the beam (and shortly after the yielding of the longitudinal bars), the width of the main crack (not always the first one) increases very rapidly and causes the longitudinal bars to pullout from the concrete, resulting in a reduction of the value of the applied torsional moment. At the end of the test, all deformations take place at the main crack, where the rest of the beam at this stage can be considered unloaded as can be seen from the photographs in Figs. 6 and 7.

C. 12   Ahmed M. Yousef

Table (2): Summary of test results.

Beam	At Cracking		At Ultimate		Predicted Cracking Torsional Strength T_{crPRE} (Eq. 1) kN.m	$\dfrac{T_{crEXP}}{T_{crPRE}}$	Proposed Cracking Torsional Strength T_{crPRO} kN.m	$\dfrac{T_{crEXP}}{T_{crPRO}}$
	T_{crEXP} kN.m	Twist Deg/m	T_{uEXP} kN.m	Twist Deg/m				
DBTN1	12.30	0.75	22.80	8.00	4.92	2.50	5.97	2.06
DBTN2	11.70	1.00	24.00	9.00	4.92	2.38	5.97	1.96
DBTN3	12.90	1.00	24.60	8.50	4.92	2.62	5.97	2.16
DBTN4	12.30	1.00	25.80	9.00	4.92	2.50	5.97	2.06
DBTN5	10.50	1.25	23.40	7.00	4.92	2.13	5.97	1.76
DBTN6	9.20	1.25	24.00	7.50	4.92	1.87	5.97	1.54
DBTN7	7.40	1.50	17.20	6.50	4.92	1.50	5.97	1.24
DBTH1	20.30	1.00	26.40	8.00	7.66	2.65	9.28	2.19
DBTH2	20.90	1.25	27.70	8.50	7.66	2.73	9.28	2.25
DBTH3	20.90	1.00	28.30	7.50	7.66	2.73	9.28	2.19
DBTH4	20.30	1.25	30.10	8.50	7.66	2.65	9.28	2.25
DBTH5	16.60	1.50	25.80	9.00	7.66	2.17	9.28	1.79
DBTH6	16.00	1.50	27.10	9.00	7.66	2.09	9.28	1.72
DBTH7	12.30	1.25	21.50	8.50	7.66	1.61	9.28	1.33

Fig. (6): Photographs of the crack patterns of some the tested NSC and HSC deep beams with L/h=1.0.

Fig. (7): Photographs of the crack patterns of the tested NSC and HSC deep beams with *L/h*=2.0.
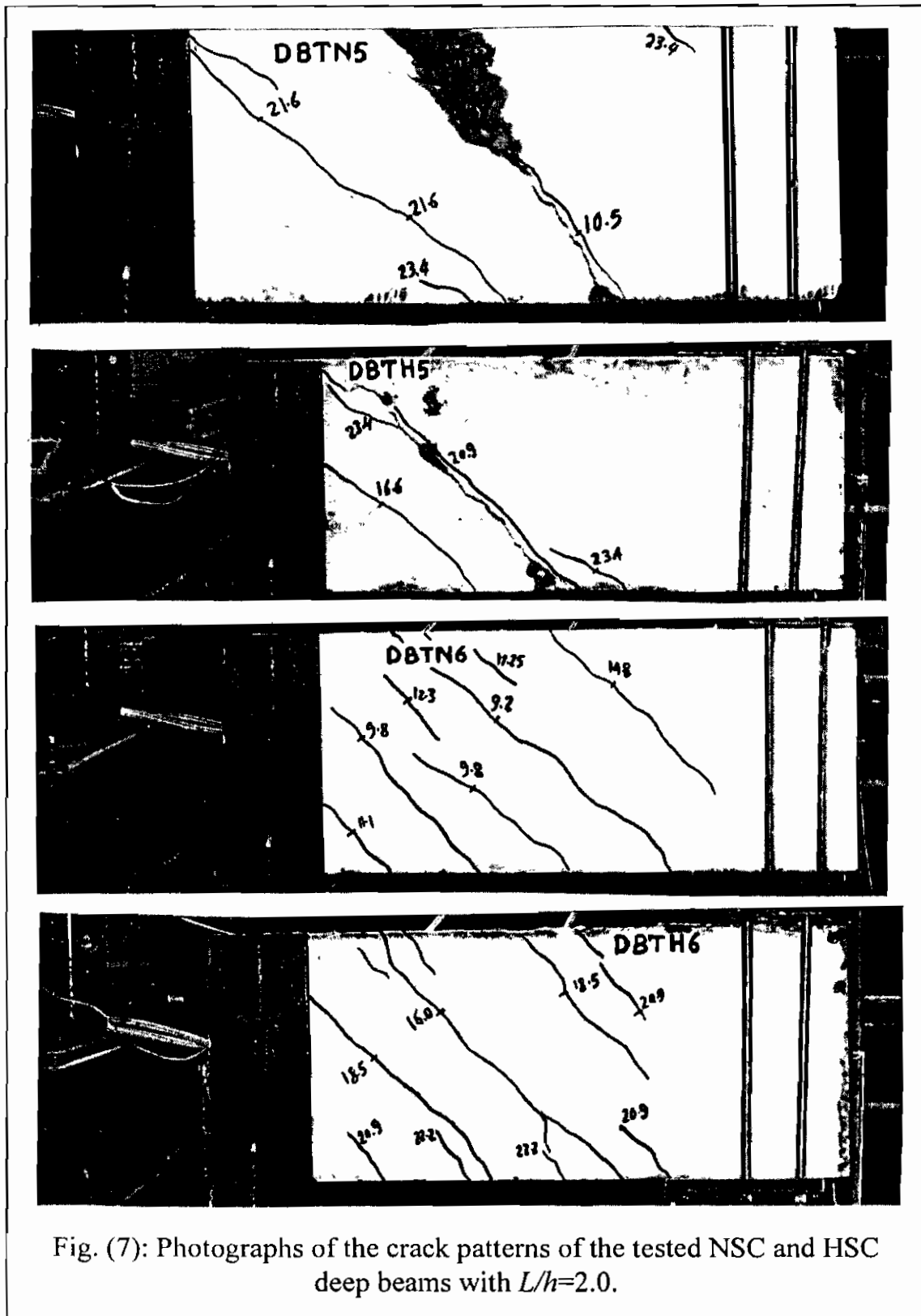
4.3 Applied Torsional Moment-Twist Relationships

The experimental torsional moment versus the angle of twist relationships for some of the tested HSC and NSC deep beams are shown in Fig. 8. These curves are approximately linear up to cracking and thereafter become nonlinear with a large drop in the torsional stiffness (as represented by the slope of the curve). Comparing the recorded torsional moment-twist relationships for similar NSC and HSC beams showed that increasing the concrete strength reduces the angle of twist for different ratios of transverse and longitudinal reinforcement. Increasing the transverse reinforcement ratio did not have considerable effect on the applied torsional moment-angle twist relationships. In addition, the torsional postcracking stiffness increases as f_c' increases for the same L/h ratio as can be seen from Fig. 8a to 8c. The effect of L/h ratio on the torsional moment-twist relationships can be seen from Fig. 8d. Increasing the L/h ratio from 1 to 3, for the similar deep beams, reduces considerably the torsional postcracking stiffness as can be seen for beams DBTH2, DBTH5 and DBTH7.
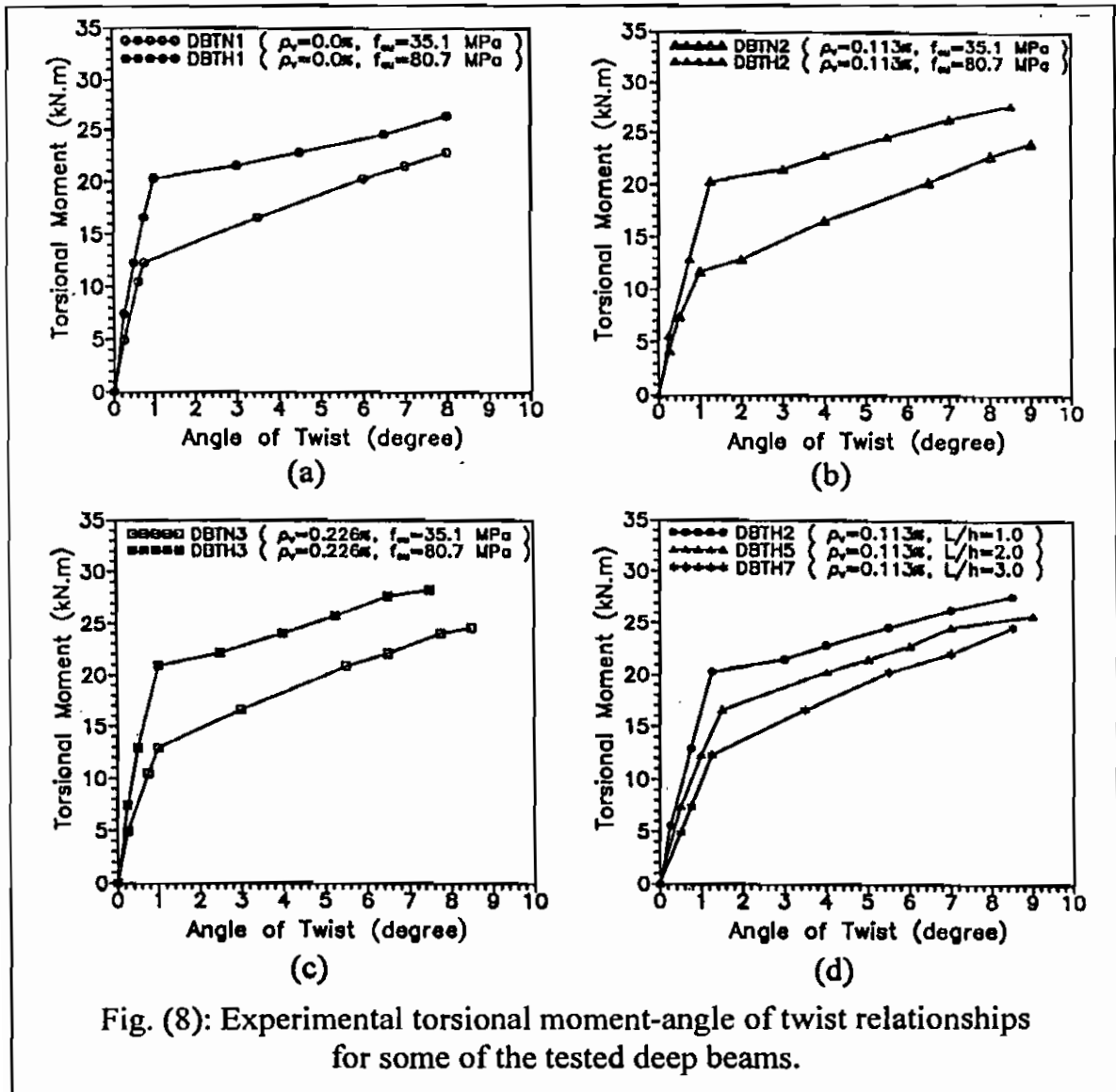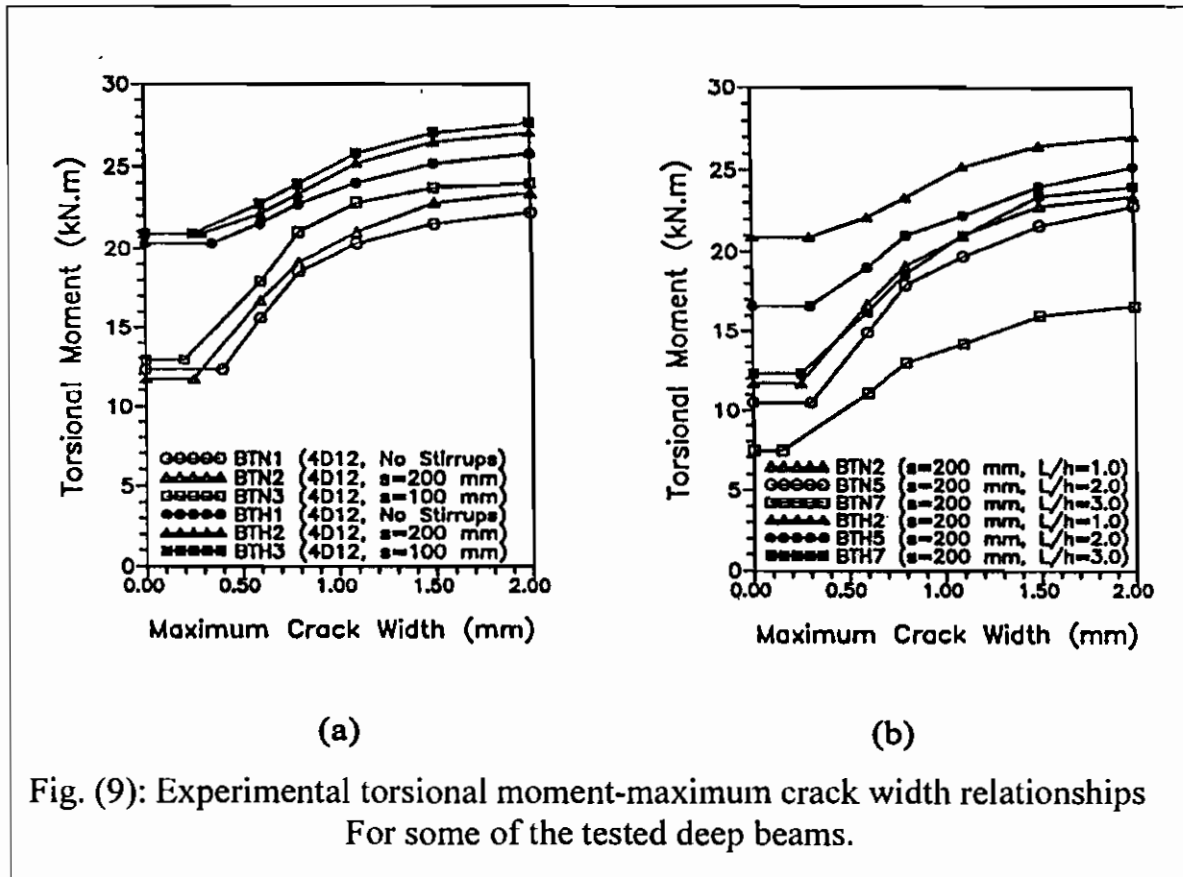

Fig. (8): Experimental torsional moment-angle of twist relationships for some of the tested deep beams.

4.4 Applied Torsional Moment-Crack Width Relationships

A plot of the applied torsional moment versus the maximum crack width for the tested NSC and HSC deep beams are shown in Fig. 9. In general, the spiral torsional cracks were relatively wide (about 0.10 mm) immediately after their formations. The cracks grew rapidly with increasing the applied torsional moments. For the same L/h ratio, the development of the major spiral torsional crack of NSC deep beams was considerably faster than that of the similar HSC deep beams as can be seen from Fig. 9a. The effect of transverse reinforcement on the development of diagonal cracks of the tested NSC and HSC deep beams can be easily noticed from the difference between deep beams with the same longitudinal reinforcement and different ratios of transverse reinforcement.

For deep beams tested at the same L/h ratio in Fig. 9a, it can be seen that the development of the major spiral torsional crack in deep beam DBTH2 with s equals to 200 mm ($\rho_v\%= 0.113$), was faster than that of the similar deep beam BTH3 but with s equals to 100 mm ($\rho_v\%= 0.226$). Increasing the corner longitudinal reinforeement ratio or the addition of skin bars for the NSC and HSC deep beams did not have observed effect on the progress of the spiral torsional cracks. For the tested HSC and NSC deep beams with the same longitudinal and web reinforcement but with different L/h ratio (L/h = 1,2 and 3), it can be seen from Fig. 9b that, the lower the L/h ratio the slower the spiral crack development.

(a)   (b)

Fig. (9): Experimental torsional moment-maximum crack width relationships For some of the tested deep beams.

5. COMPARISON OF TEST RESULTS WITH THE TORSION PROVISIONS

The equation used by the NZS 3101-95, ACI 318-02 building code and ECCS-2001 for calculating the cracking torsional strength for reinforced concrete deep beams (Eq. 1) have been used to predict the cracking torsional strength T_{crPRE} of the tested beams (7 NSC deep beams+7 HSC deep beams). A comparison between the recorded experimental cracking strength T_{crEXP} and the predicted values T_{crPRE} are given in Table 2. The mean value of the ratio T_{crEXP} to T_{crPRE} for NSC and HSC deep beams is 2.21 and 2.38, respectively, with a coefficient of variation of 0.170 and 0.167, respectively . This shows that the equation used by the three mentioned codes underestimates the cracking strength of NSC and HSC deep beams subjected to pure torsion. A little modification to Equation 1 can be proposed by changing the value 0.33 to be 0.40. The calculated values of the cracking torsional strength of the tested deep beams using the proposed equation T_{crPRO} is given in Table 2. The mean value of the ratio (T_{crEXP} / T_{crPRO}) for NSC and HSC deep beams is 1.83 and 1.96, respectively, with a coefficient of variation of 0.169 and 0.168, respectively.

The torsion design methods for reinforced concrete beams according to the provisions of the ACI 318-02 building code, NZS 3101-95, ECCS-2001 and EC-2 are used to predict the ultimate torsional strength of the NSC and HSC deep beams of this study depending on the ultimate concrete strength T_{uc}, ultimate strength of stirrups T_{ut} and ultimate strength of longitudinal bars T_{ul}, respectively, as can be seen from Table 3 and Table 4. The maximum ultimate torsional moment predicted by the studied codes T_{uMAXP} are also given in Table 3 and 4. The calculated values of the angle θ between the concrete struts and the

longitudinal axis of the beam (using Eq. 7) are also summarized in Table 3. It can be seen that, although all the studied codes adopted the same thin-walled tube and truss model the calculated torsional strength for the tested NSC and HSC deep beams according to these codes differ markedly. Under-reinforced beam according to one code maybe over-reinforced or partially over-reinforced according to another code. The great differences in the predicted values of the torsional moment strength of the tested NSC and HSC deep beams are due to the great differences in the values of the angle θ adopted by each code. According to NZS 3101-95 and ECCS-2001 the angle θ is taken equal to 45 deg. According to the ACI 318-02 the angle θ is taken between 30 deg and 60 deg, while according to the EC-2 the angle θ is taken between 21.8 and 68.2 deg. The ACI 318-02 code allows also that θ can be taken equal 45 deg for nonprestressed members. For this case, the provisions of ACI 318-02 will be greatly similar to that of ECCS-2001. The value of the angle θ considerably affects the predicted values of the ultimate torsional strength depending on the ultimate strength of stirrups and ultimate strength of longitudinal bars. It can be seen also from Tables 3 and 4 that, for the tested NSC and HSC deep beams, the equations used by the ACI 318-02, NZS 3101-95 and ECCS-2001 underestimate the ultimate torsional strength of the concrete T_{uc}, while the equations used by the EC-2 predict reasonably these values. This can be attributed to the relatively small limits put by the ACI 318-02 and ECCS-2001 on the maximum torsional strength of concrete as can be seen from Equations 4 and 12. The NZS 3101-95 limited this value to be less than or equal to $0.2 f_c$ or 6 MPa. The limits of NZS 3101-95 are also very conservative when applied for NSC and HSC deep beams.

Table (3): Calculated torsional strength according to the ACI 318-02 code.

Beam	θ (deg) Eq. 6	ACI 318-02 (θ = 30 - 60 deg)				ACI 318-02 (θ = 45 deg)			
		T_{uc} kN.m	T_{ul} kN.m	T_{ul} kN.m	T_{uMAXP} KN.m	T_{uc} kN.m	T_{ul} kN.m	T_{ul} kN.m	T_{uMAXP} KN.m
DBTN1	-	7.46	-	6.36	7.46	7.46	-	11.01	11.01
DBTN2	24.61	7.46	4.01	6.36	7.46	7.46	2.31	11.01	11.01
DBTN3	32.95	7.46	7.14	7.14	7.46	7.46	4.63	11.01	11.01
DBTN4	17.35	7.46	4.01	14.38	14.38	7.46	2.31	24.90	24.90
DBTN5	24.61	7.46	4.01	6.36	7.46	7.46	2.31	11.01	11.01
DBTN6	32.95	7.46	7.14	7.14	7.46	7.46	4.63	11.01	11.01
DBTN7	24.61	7.46	4.01	6.36	7.46	7.46	2.31	11.01	11.01
DBTH1	-	11.61	-	6.36	11.61	11.61	-	11.01	11.61
DBTH2	24.61	11.61	4.01	6.36	11.61	11.61	2.31	11.01	11.61
DBTH3	32.95	11.61	7.14	7.14	11.61	11.61	4.63	11.01	11.61
DBTH4	17.35	11.61	4.01	14.38	14.38	11.61	2.31	24.90	24.90
DBTH5	24.61	11.61	4.01	6.36	11.61	11.61	2.31	11.01	11.61
DBTH6	32.95	11.61	7.14	7.14	11.61	11.61	4.63	11.01	11.61
DBTH7	24.61	11.61	4.01	6.36	11.61	11.61	2.31	11.01	11.61

Table (4): Calculated torsional strength according to three of the studied codes.

Beam	ECCS-2001				NZS 3101-95				EC-2			
	T_{uc} kN.m	T_{ul} kN.m	T_{ul} kN.m	T_{uMAXP} kN.m	T_{uc} KN.m	T_{ul} kN.m	T_{ul} kN.m	T_{uMAXP} kN.m	T_{uc} kN.m	T_{ul} kN.m	T_{ul} kN.m	T_{uMAXP} kN.m
DBTN1	6.46	-	9.57	9.57	6.63	-	10.52	10.52	6.87	-	4.41	6.87
DBTN2	6.46	2.01	9.57	9.57	6.63	2.05	10.52	10.52	7.55	5.04	5.05	7.55
DBTN3	6.46	4.02	9.57	9.57	6.63	4.10	10.52	10.52	9.09	7.14	7.14	9.09
DBTN4	6.46	2.01	21.65	21.65	6.63	2.05	22.55	22.55	6.87	5.78	9.96	9.96
DBTN5	6.46	2.01	9.57	9.57	6.63	2.05	10.52	10.52	7.55	5.04	5.05	7.55
DBTN6	6.46	4.02	9.57	9.57	6.63	4.10	10.52	10.52	9.09	7.14	7.14	9.09
DBTN7	6.46	2.01	9.57	9.57	6.63	2.05	10.52	10.52	6.87	5.04	5.05	6.87
DBTH1	10.71	-	9.57	10.71	6.76	-	10.52	10.52	13.54	-	4.41	13.54
DBTH2	10.71	2.01	9.57	10.71	6.76	2.05	10.52	10.52	14.89	5.04	5.05	14.89
DBTH3	10.71	4.02	9.57	10.71	6.76	4.10	10.52	10.52	17.92	7.14	7.14	17.92
DBTH4	10.71	2.01	21.65	21.65	6.76	2.05	22.55	22.55	13.54	5.78	9.96	13.54
DBTH5	10.71	2.01	9.57	10.71	6.76	2.05	10.52	10.52	14.89	5.04	5.05	14.89
DBTH6	10.71	4.02	9.57	10.71	6.76	4.10	10.52	10.52	17.92	7.14	7.14	17.92
DBTH7	10.71	2.01	9.57	10.71	6.76	2.05	10.52	10.52	14.89	5.04	5.05	14.89

Table (5): Comparison between the experimental results and the maximum torsional strength predicted by the studied codes.

Beam	T_{uEXP} kN.m	ACI 318-02 $(\theta = 30\text{-}60 \text{ deg})$ $\dfrac{T_{uEXP}}{T_{uMAXP}}$	ACI 318-02 $(\theta = 45 \text{ deg})$ $\dfrac{T_{uEXP}}{T_{uMAXP}}$	ECCS-2001 $\dfrac{T_{uEXP}}{T_{uMAXP}}$	NZS 3101-95 $\dfrac{T_{uEXP}}{T_{uMAXP}}$	EC-2 $\dfrac{T_{uEXP}}{T_{uMAXP}}$
DBTN1	22.80	3.06	2.07	2.38	2.17	3.31
DBTN2	24.00	3.22	2.18	2.51	2.28	3.18
DBTN3	24.60	3.30	2.23	2.57	2.34	2.34
DBTN4	25.80	1.79	1.04	1.19	1.14	2.59
DBTN5	23.40	3.14	2.13	2.13	2.22	3.10
DBTN6	24.00	3.22	2.18	2.45	2.28	2.64
DBTN7	17.20	2.31	1.56	1.80	1.63	2.50
DBTH1	26.40	2.27	2.27	2.46	2.51	1.95
DBTH2	27.70	2.39	2.39	2.59	2.63	1.86
DBTH3	28.30	2.44	2.44	2.64	2.69	1.58
DBTH4	30.10	2.09	1.21	1.39	1.33	2.22
DBTH5	25.80	2.22	2.22	2.41	2.45	1.73
DBTH6	27.10	2.33	2.33	2.53	2.58	1.51
DBTH7	21.50	1.85	1.85	2.01	2.04	1.44
Mean / C.O.V (NSC Deep Beams)		2.86 / 0.084	1.91 / 0.218	2.20 / 0.218	2.01 / 0.208	2.81 / 0.125
Mean / C.O.V (HSC Deep Beams)		2.23 / 0.188	2.10 / 0.193	2.29 / 0.181	2.32 / 0.194	1.76 / 0.145

As can be seen from Table 5, the predictions of the ultimate torsional strength using ACI 318-02 provisions are very conservative for the tested NSC and HSC deep beams. The mean of the ratio (T_{uEXP}/T_{uMAXP}) for the tested NSC and HSC deep beams of the case of ACI 318-02 code is 2.86 and 2.23, respectively, with a coefficient of variation of 0.188 and 0.084, respectively. This showed that, the applications of the equations of this code for NSC deep beams is more conservative than that of HSC beams. Using a value of the angle θ equal 45 deg by ACI 318-02 code will lead to a level of conservation for the tested NSC and HSC deep beams which is less than that when the angle θ is taken between 30 and 60 deg.

According to EC-2, the ratio (T_{uEXP}/T_{uMAXP}) for the tested HSC deep beams is considerably less than that of the tested NSC deep beams. Using a value of the angle θ as recommended by this code leads to a maximum predicted value of the torsional moment which is based on the ultimate strength of the concrete T_{uc} (for all the tested HSC deep beams and all the tested NSC deep beams except DBTN4). For the ECCS-2001, NZS 3101-95 and ACI 318-02 (θ =45) codes, the conservatism reduces considerably with increasing the amount of torsional longitudinal bars for the tested NSC and HSC deep beams (DBTN4 and DBTH4). This shows that, for these codes, using the torsional strength of the deep beams based on the strength of the longitudinal bars may lead to unconservative results, especially for NSC deep beams. Consequently, for design purposes, the design ultimate torsional moment should be kept less than the ultimate torsional strength based on the ultimate torsional concrete strength or the ultimate torsional strength of the stirrups.

6. CONCLUSIONS

Based on the results of this study, the following can be concluded:

1. The overall behavior of HSC deep beams in torsion is generally similar to that of the NSC beams. Increasing the concrete compressive strength of the tested beams from f_{cu} =35.1 MPa to 80.7 MPa increases considerably the cracking torsional strength (by about 33-88%) and slightly the ultimate torsional strength (by about 15-25%). The failure of HSC deep beams under pure torsion is similar to that of the NSC beams and mainly controlled by the strain in the longitudinal corner bars of the beam regardless of the amount of the stirrups.

2. The reserve in the torsional strength of the HSC deep beams after cracking is considerably less than that of the similar NSC deep beams. The cracking torsional strength of the NSC and HSC deep beams is 38-54% and 57-77% of the measured ultimate torsional strength, respectively.

3. The tested span to total height ratio (L/h) have considerable effect on the cracking and the ultimate torsional strength of NSC and HSC beams. Increasing the L/h ratio from 1 to 3 reduced the cracking torsional strength of NSC and HSC deep beams by about 37% and 41%, respectively, and the ultimate torsional strength by about 28% and 22%, respectively.

4. Although all the four codes examined in this study adopted the same thin-walled tube model, the torsional design equations differ markedly. However, the design torsional strength equations of the four codes were safe and conservative when applied to NSC and HSC deep beams.

5. The predictions of the ultimate torsional strength of the deep beams according to the method of ACI 318-02 and using a value of the angle between the concrete struts and the longitudinal axis of the beam θ equal to 45 deg may give a conservative results less than that calculated using this angle between 30 and 60 deg.

6. The calculation of the ultimate torsion strength using the angle θ equal to 45 deg and depending on the amount of the longitudinal bars according to ACI 318-02, NZS 3101-95 and ECCS-2001 may lead to unsafe results when applied to NSC and HSC deep beams.

REFERENCES

1. ACI Committee 363, " State-of-the-Art Report on High-Strength Concrete ", ACI 363R-92, American Concrete Institute, Mich., 1992, 55 p.

2. ACI-ASCE Committee 326 (1962), " Shear and Diagonal Tension," ACI Journal, Proceedings V. 59, No.1, pp. 1-30 and No. 2, 1962, pp. 277-334.

3. Standards Association of New Zealand, "Code of Practice for the Design of Concrete Structures (NZS 3101)," Part 1& Part 2, Wellington, New Zealand, 1995.

4. Commission of the European Communities, " Eurocode No. 2: Design of Concrete Structures," Part 1: General Rules and Rules for Buildings, October, 1990.

5. ACI Committee 318, " Building Code Requirements for Reinforced Concrete and Commentary (ACI 318-02)," American Concrete Institute, 2002.

6. Ministry of Housing, Utilities and Urban Communities, " Egyptian Code for Design and Construction of Reinforced Concrete Structures (ECCS 203-2001)," Cairo, 2001.

7. Rahal, K. N., and Collins, M. P., " Experimental Evaluation of ACI and AASHTO-LRFD Design Provisions for Combined Shear and Torsion," ACI Structural Journal, Vol. 100, No. 3, May-June 2003, pp. 277-282.

8. Ashour, A. A., Samman, T. A., and Radain, T. A., " Torsional Behavior of Reinforced High-Strength Concrete Deep Beams," ACI Structural Journal, Vol. 96, No. 6, 1999, pp. 1049-1058.